

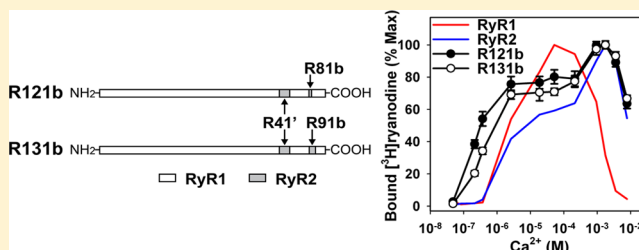
# Two Regions of the Ryanodine Receptor Calcium Channel Are Involved in $\text{Ca}^{2+}$ -Dependent Inactivation

Angela C. Gomez and Naohiro Yamaguchi\*

Department of Regenerative Medicine and Cell Biology, Medical University of South Carolina, and Cardiac Signaling Center, University of South Carolina, Medical University of South Carolina, and Clemson University, Charleston, South Carolina 29425, United States

## Supporting Information

**ABSTRACT:** Skeletal (RyR1) and cardiac muscle (RyR2) isoforms of ryanodine receptor calcium channels are inhibited by millimolar  $\text{Ca}^{2+}$ , but the affinity of RyR2 for inhibitory  $\text{Ca}^{2+}$  is  $\sim 10$  times lower than that of RyR1. Previous studies demonstrated that the C-terminal quarter of RyR has critical domain(s) for  $\text{Ca}^{2+}$  inactivation. To obtain further insights into the molecular basis of regulation of RyRs by  $\text{Ca}^{2+}$ , we constructed and expressed 18 RyR1–RyR2 chimeras in HEK293 cells and determined the  $\text{Ca}^{2+}$  activation and inactivation affinities of these channels using the  $[\text{H}^3]$ -ryanodine binding assay. Replacing two distinct regions of RyR1 with corresponding RyR2 sequences reduced the affinity for  $\text{Ca}^{2+}$  inactivation. The first region (RyR2 amino acids 4020–4250) contains two EF-hand  $\text{Ca}^{2+}$  binding motifs (EF1, amino acids 4036–4047; EF2, amino acids 4071–4082), and the second region includes the putative second transmembrane segment (S2). A RyR1–backbone chimera containing only EF2 from RyR2 had a modest (not significant) change in  $\text{Ca}^{2+}$  inactivation, whereas another chimera channel carrying only EF1 from RyR2 had a significantly reduced level of  $\text{Ca}^{2+}$  inactivation. The results suggest that EF1 is a more critical determinant for RyR inactivation by  $\text{Ca}^{2+}$ . In addition, activities of the chimera carrying RyR2 EF-hands were suppressed at  $10\text{--}100\ \mu\text{M}\ \text{Ca}^{2+}$ , and the suppression was relieved by  $1\ \text{mM}\ \text{Mg}^{2+}$ . The same effects have been observed with wild-type RyR2. A mutant RyR1 carrying both regions replaced with RyR2 sequences (amino acids 4020–4250 and 4560–4618) showed a  $\text{Ca}^{2+}$  inactivation affinity comparable to that of RyR2, indicating that these regions are sufficient to confer RyR2-type  $\text{Ca}^{2+}$ -dependent inactivation on RyR1.



Skeletal and cardiac muscle  $\text{Ca}^{2+}$  release channels, also known as ryanodine receptors (RyRs), are responsible for the release of  $\text{Ca}^{2+}$  from the sarcoplasmic reticulum (SR), an intracellular  $\text{Ca}^{2+}$  storage compartment, during muscle excitation.<sup>1</sup> Both skeletal (RyR1) and cardiac (RyR2) isoforms of RyR are homotetramers of a 560 kDa subunit and are regulated by various molecules and proteins, including  $\text{Ca}^{2+}$ ,  $\text{Mg}^{2+}$ , ATP, protein kinases and phosphatases, and  $\text{Ca}^{2+}$  binding proteins such as calmodulin.<sup>2–4</sup>

Intracellular  $\text{Ca}^{2+}$  concentrations dynamically change from submicromolar to micromolar levels during muscle excitations, which regulate RyR ion channels by positive and negative feedback mechanisms. Mechanical interaction (RyR1) or a small influx of  $\text{Ca}^{2+}$  (RyR2) triggers RyR channels to open, and released  $\text{Ca}^{2+}$  at a micromolar level possibly allows neighbor RyRs to open by a positive feedback mechanism. Mechanisms for closing RyR channels are not well-understood. Several possibilities include  $\text{Ca}^{2+}$ -dependent inactivation through a direct or indirect mechanism, time-dependent inactivation, and depletion of SR  $\text{Ca}^{2+}$  stores.  $\text{Ca}^{2+}$  binding domains were characterized using truncated and full-length RyR forms.<sup>5–10</sup> Point mutations in RyR2 Glu3987 or RyR3 Glu3885 (corresponding to RyR1 Glu4032) drastically reduced the level of  $\text{Ca}^{2+}$ -dependent activation of the channel, which

indicated the location of a  $\text{Ca}^{2+}$  activation site in RyRs.<sup>6,7</sup> Other experiments have revealed two EF-hand  $\text{Ca}^{2+}$  binding sites in RyR1 (RyR1 amino acids 4081–4127).<sup>8–10</sup> Using truncated forms of proteins, the affinity for  $\text{Ca}^{2+}$  was measured to be  $60\ \mu\text{M}$  to  $3.8\ \text{mM}$ , a range that exceeds the affinities for  $\text{Ca}^{2+}$  activation. The results suggest that the region may be involved in inactivation of RyRs by millimolar levels of  $\text{Ca}^{2+}$ . Single-channel studies indicated that released  $\text{Ca}^{2+}$  through RyR inhibits the same RyR channel;<sup>11,12</sup> therefore, it is probable that cytoplasmic  $\text{Ca}^{2+}$  concentrations reach millimolar levels locally around the inactivation site of RyRs. RyR1 is inhibited by  $\sim 1\ \text{mM}\ \text{Ca}^{2+}$ , but  $\sim 10$ -fold higher concentrations are required to inhibit RyR2 channel activities.<sup>13,14</sup> Therefore, RyR1–RyR2 chimera channels were constructed and analyzed to identify the  $\text{Ca}^{2+}$  inactivation site in RyRs, revealing that an  $\sim 1300$ -amino acid sequence in the C-terminus is responsible for inactivation.<sup>15,16</sup>

Another physiological divalent cation,  $\text{Mg}^{2+}$ , is well-known to inhibit RyR activities. Two possible mechanisms of inhibitory

Received: November 26, 2013

Revised: February 6, 2014

Published: February 12, 2014

effects by  $Mg^{2+}$  have been recognized. (1)  $Mg^{2+}$  competes off  $Ca^{2+}$  at the  $Ca^{2+}$  activation site (A site), and (2)  $Mg^{2+}$  binds to a lower-affinity  $Ca^{2+}$  inactivation site (I site) to facilitate its inhibitory effects.<sup>17,18</sup> In addition,  $Mg^{2+}$  was reported to “activate” RyR2 at 10–100  $\mu M$   $Ca^{2+}$ .<sup>19</sup> This activation was observed in rat ventricular SR and rabbit recombinant RyR2, but not in rabbit ventricular SR. Further,  $Mg^{2+}$  activation has never been reported on RyR1.

Here, we pursued the previous studies using RyR1–RyR2 chimera channels<sup>15,16</sup> to improve our understanding of the structural basis of differential regulation of RyR1 and RyR2 by  $Ca^{2+}$  and  $Mg^{2+}$ . We constructed 18 chimeras and determined their  $Ca^{2+}$ -dependent channel activities and  $Mg^{2+}$ -dependent regulation. Two distinct regions were found to be involved in isoform-specific  $Ca^{2+}$ -dependent inhibition of RyR channels. Moreover, we found that a RyR1–RyR2 chimera carrying the RyR2 EF-hand  $Ca^{2+}$  binding domain was activated by  $Mg^{2+}$ .

## MATERIALS AND METHODS

**Materials.** [ $^3H$ ]Ryanodine was obtained from PerkinElmer (Waltham, MA) and unlabeled ryanodine from Calbiochem (La Jolla, CA). Protease inhibitors were obtained from Roche (Indianapolis, IN) and Sigma-Aldrich (St. Louis, MO) and human embryonic kidney (HEK) 293 cells from American Type Culture Collection. Full-length wild-type RyR1 cDNA was provided by G. Meissner (University of North Carolina, Chapel Hill, NC). Full-length wild-type RyR2 and R1 chimera cDNAs were provided by J. Nakai (Saitama University, Saitama, Japan).

**Construction of RyR cDNAs.** Full-length rabbit RyR1 and RyR2 cDNAs were cloned into mammalian expression vectors pCMV5 and pCIneo, respectively. RyR1–RyR2 chimera cDNAs were constructed by using common restriction enzyme sites or by introducing new restriction enzyme sites by site-directed mutagenesis or by polymerase chain reaction. Single- and multiple-base changes and deletions were introduced by *Pfu*-turbo polymerase-based chain reaction, using mutagenic oligonucleotides and the QuikChange site-directed mutagenesis kit (Agilent, Santa Clara, CA). Complete mutated DNA fragments amplified by PCR were confirmed by DNA sequencing. Sequences and numbering were described previously.<sup>20,21</sup>

**Expression of Full-Length RyRs in HEK293 Cells.** RyR cDNAs were transiently expressed in HEK293 cells with FuGene6 (Promega) according to the manufacturer’s instruction. Cells were maintained at 37 °C and 5%  $CO_2$  in high-glucose Dulbecco’s modified Eagle’s medium containing 10% fetal bovine serum and were plated the day before transfection. For each 10 cm tissue culture dish, 3.5  $\mu g$  of cDNA was used, and cells were harvested 48 h after transfection. To prepare crude membrane fractions, cells were homogenized with 0.3 M sucrose, 150 mM KCl, 20 mM imidazole (pH 7.0), 0.1 mM ethylene glycol tetraacetic acid (EGTA), 1 mM glutathione (oxidized), and protease inhibitors. Homogenates were centrifuged for 45 min at 100000g, and pellets were resuspended in the aforementioned buffer without EGTA and glutathione. Expression levels of RyRs in each transfection were determined by  $B_{max}$  measurements of binding of [ $^3H$ ]ryanodine to the crude membrane fractions (see below).

**[ $^3H$ ]Ryanodine Binding.** [ $^3H$ ]Ryanodine binding experiments were performed with crude membrane fractions as described previously.<sup>22,23</sup> Unless otherwise indicated, membranes were incubated with 2.5 nM [ $^3H$ ]ryanodine in 20 mM

HEPES (pH 7.4), 0.15 M sucrose, 200 mM KCl, 0.3 mM glutathione (oxidized), protease inhibitors, and the indicated  $Ca^{2+}$  and  $Mg^{2+}$  concentrations. Nonspecific binding was assessed using a 1000–2000-fold excess of unlabeled ryanodine. Effects of  $Mg^{2+}$  on channel activity at 100  $\mu M$   $Ca^{2+}$  (Figures 2C and 5C) were measured in the absence of glutathione. After 20 h, samples were diluted with 6 volumes of ice-cold water and placed on Whatman GF/B filters preincubated with 2% polyethyleneimine in water. Filters were washed three times with 5 mL of an ice-cold 100 mM KCl, 1 mM KPIPES (pH 7.0) solution. The radioactivity remaining on the filters was determined by liquid scintillation counting to obtain bound [ $^3H$ ]ryanodine. In parallel experiments, the  $B_{max}$  of [ $^3H$ ]ryanodine binding was determined by incubating homogenates for 4–5 h with a nearly saturating concentration of 20 nM [ $^3H$ ]ryanodine in 20 mM imidazole (pH 7.0), 0.6 M KCl, protease inhibitors, and 0.1 mM  $Ca^{2+}$ . All experiments were performed at room temperature (22–24 °C).

**Biochemical Assays and Data Analysis.** Free  $Ca^{2+}$  concentrations were obtained by including the appropriate amounts of  $Ca^{2+}$  and EGTA in the solutions as determined using the stability constants and a computer program published by Shoenmakers et al.<sup>24</sup> Free  $Ca^{2+}$  concentrations of  $\geq 1 \mu M$  were verified with the use of a  $Ca^{2+}$  selective electrode.

Results are given as means  $\pm$  the standard error (SE). The significance of the differences in data among three or more groups ( $p < 0.05$ ) was determined using one-way analysis of variance (ANOVA) followed by Tukey’s test. Otherwise, a Student’s *t* test was used.

## RESULTS

**Two Regions in the C-Terminal Quarter of RyRs Are Involved in  $Ca^{2+}$ -Dependent Inactivation.** Both RyR1 and RyR2 have similar affinities at the micromolar level for  $Ca^{2+}$  activation, but RyR2 has an  $\sim 10$ -fold lower affinity for  $Ca^{2+}$  inhibitory effect than RyR1.<sup>13,14</sup> Studies with RyR1–RyR2 chimera channels demonstrated that the C-terminal quarter of RyR is crucial for this difference.<sup>15,16</sup>

In this study, we pursued these observations by constructing and expressing 18 additional RyR1–RyR2 chimera channels. We measured the binding of [ $^3H$ ]ryanodine to crude membrane fractions of HEK293 cells expressing recombinant rabbit WT RyR1, WT RyR2, and the RyR1–RyR2 chimera channels at various  $Ca^{2+}$  concentrations. Ryanodine specifically binds to RyRs and is widely used as a probe for RyR channel activity because of its preferential binding to the open state of RyR channels.<sup>25</sup> Accordingly, we used [ $^3H$ ]ryanodine binding as a measure of the apparent affinity for  $Ca^{2+}$ -dependent activation and inactivation. As shown in Figure 1A, we observed an atypical bell-shaped curve with WT RyR2; the curve had a plateau level at 10–100  $\mu M$   $Ca^{2+}$ . This has already been reported in microsomes of rat heart and recombinant rabbit RyR2.<sup>19</sup> It was also reported that  $\sim 1$  mM  $Mg^{2+}$  restored the normal bell-shaped  $Ca^{2+}$ -dependent curve of recombinant RyR2 with activation at 10–100  $\mu M$   $Ca^{2+}$ . We confirmed the effect of 1 mM  $Mg^{2+}$  on the  $Ca^{2+}$ -dependent regulation of rabbit recombinant RyR2, but we did not observe the suppression of WT RyR1 at 10–100  $\mu M$   $Ca^{2+}$  in the absence of  $Mg^{2+}$  (Figure 1A). In this study, we characterized some RyR1–RyR2 chimera channels in the presence of 1 mM  $Mg^{2+}$  for comparison with WT RyR1 and WT RyR2 (see below).

In previous studies, RyR1 channels carrying the C-terminal quarter of RyR2 [R1 chimera (Figure 1B)] showed essentially

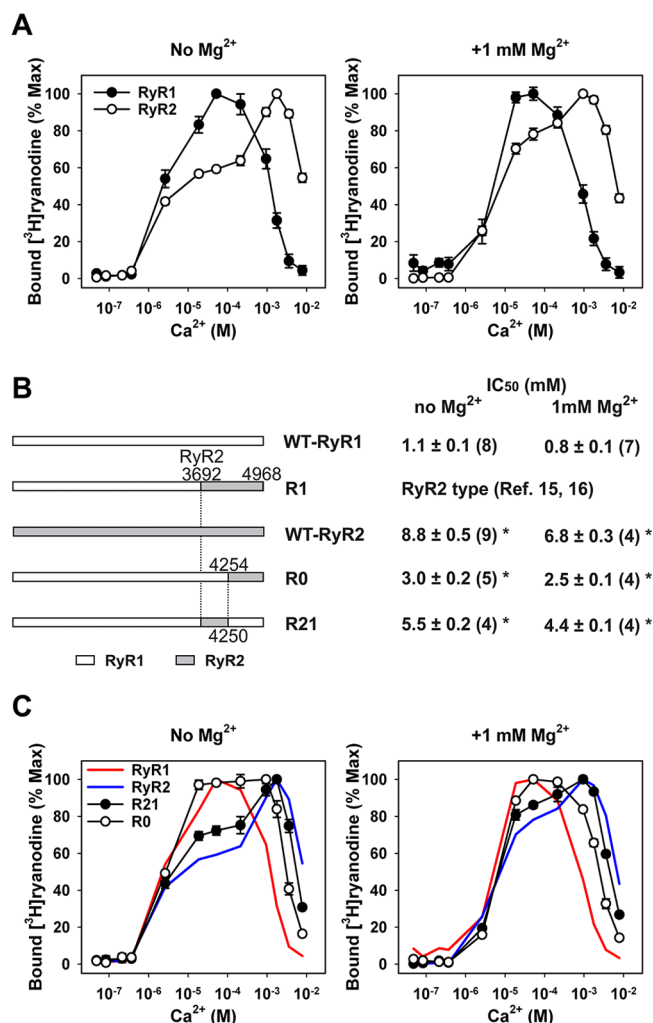


**Figure 1.** Two regions are involved in isoform-specific  $Ca^{2+}$ -dependent inactivation of RyRs. (A)  $Ca^{2+}$ -dependent changes in the activities of WT RyR1 (●) and WT RyR2 (○) were measured in [ $^3H$ ]ryanodine binding assays in the absence (left) or presence (right) of 1 mM  $Mg^{2+}$ . Data are means  $\pm$  SE ( $n = 4$ –9). (B) Schematic of R21 and R0 chimeras together with the R1 chimera, which was shown to have RyR2-type  $Ca^{2+}$ -dependent inactivation.<sup>15,16</sup> IC<sub>50</sub> values are means  $\pm$  SE of the number of experiments indicated in parentheses. \* $p < 0.05$  compared with WT RyR1 (ANOVA followed by Tukey's test among four groups). (C)  $Ca^{2+}$ -dependent regulation of R21 (●) and R0 (○) chimeras in the absence (left) or presence (right) of 1 mM  $Mg^{2+}$ . Solid red and blue lines represent mean values of WT RyR1 and WT RyR2, respectively, from panel A. Data are means  $\pm$  SE ( $n = 4$ –5).

the same  $Ca^{2+}$  inactivation affinities as WT RyR2.<sup>15,16</sup> In our study, we confirmed impaired  $Ca^{2+}$ -dependent inactivation of R1 chimera (Figure S1 of the Supporting Information). The IC<sub>50</sub> values of the R1 chimera are >10-fold greater than that of WT RyR1 and even slightly higher than that of WT RyR2. To further narrow the critical domain for  $Ca^{2+}$ -dependent inactivation of RyRs, we first divided the C-terminal quarter of RyR2 into two segments and determined  $Ca^{2+}$ -dependent regulation of the two chimera channels (Figure 1B).  $Ca^{2+}$  inactivation affinities for both the R21 chimera (RyR1 amino acids 1–3725 and 4299–5038; RyR2 amino acids 3692–4250) and the R0 chimera (RyR1 amino acids 1–4301; RyR2 amino acids 4254–4968) were between those of WT RyR1 and WT RyR2 (Figure 1C).  $Ca^{2+}$  activation affinities of R21 and R0 chimeras were comparable with that of WT RyR1 (Table 1).

**Table 1.** Activation of RyR1–RyR2 Chimera Channels by  $Ca^{2+}$ <sup>a</sup>

chimera	EC <sub>50</sub> ( $\mu$ M)	
	no $Mg^{2+}$	1 mM $Mg^{2+}$
WT RyR1	2.9 $\pm$ 0.6 (8)	5.4 $\pm$ 0.6 (7)
R0	2.9 $\pm$ 0.1 (5)	6.8 $\pm$ 0.1 (4)
R21	4.3 $\pm$ 0.5 (4)	7.3 $\pm$ 0.4 (4)
R41	1.6 $\pm$ 0.1 (4)	4.3 $\pm$ 0.8 (4)
R51	1.8 $\pm$ 0.1 (5)	4.0 $\pm$ 0.7 (4)
R41'	1.9 $\pm$ 0.1 (4)	3.0 $\pm$ 0.2 (5)
R51'	1.6 $\pm$ 0.2 (6)	3.8 $\pm$ 0.5 (4)
R61	1.6 $\pm$ 0.3 (5)	ND <sup>b</sup>
R71	1.6 $\pm$ 0.2 (4)	ND <sup>b</sup>
R81a	2.2 $\pm$ 0.4 (4)	ND <sup>b</sup>
R81b	1.2 $\pm$ 0.2 (4)	ND <sup>b</sup>
R81c	4.3 $\pm$ 1.1 (5)	ND <sup>b</sup>
R81d	1.9 $\pm$ 0.3 (5)	ND <sup>b</sup>
R91a	1.0 $\pm$ 0.1 (4)	ND <sup>b</sup>
R91b	1.8 $\pm$ 0.1 (6)	ND <sup>b</sup>
R101a	1.7 $\pm$ 0.1 (4)	ND <sup>b</sup>
R101b	1.5 $\pm$ 0.1 (4)	ND <sup>b</sup>
R121b	0.5 $\pm$ 0.1 (5)	ND <sup>b</sup>
R131b	1.1 $\pm$ 0.1 (5)	ND <sup>b</sup>
WT RyR2	10.2 $\pm$ 2.8 (9)	8.0 $\pm$ 0.4 (4)

<sup>a</sup>Data are means  $\pm$  SE of the number of experiments shown in parentheses. <sup>b</sup>Not determined.

The higher EC<sub>50</sub> of WT RyR2 is likely due to the suppression of activities at 10–100  $\mu$ M  $Ca^{2+}$  in the absence of  $Mg^{2+}$ . Apparent IC<sub>50</sub> values of  $Ca^{2+}$  for R21 and R0 were significantly higher than that of WT RyR1 in the absence and presence of 1 mM  $Mg^{2+}$  (Figure 1B), suggesting that both regions are required for isoform-specific  $Ca^{2+}$ -dependent inactivation. We also found that activities of R21 chimera were suppressed at 10–100  $\mu$ M  $Ca^{2+}$ , and the suppression was relieved by 1 mM  $Mg^{2+}$ . However, we did not observe the same trend with the R0 chimera (Figure 1C; see also Figure 2C). The results also suggest that  $Mg^{2+}$  activated recombinant WT RyR2 at 10–100  $\mu$ M  $Ca^{2+}$  through the region highlighted by the R21 chimera (RyR2 amino acids 3692–4250).

**Two EF-Hand  $Ca^{2+}$  Binding Motifs Involved in  $Ca^{2+}$ -Dependent Inactivation.** We further narrowed the regions that were included in isoform-specific  $Ca^{2+}$  inactivation of RyR by subdividing the RyR2 region highlighted in R21 chimera channels (Figure 2A). This region contains two EF-hand  $Ca^{2+}$  binding motifs (EF1 and EF2) in tandem.<sup>8–10</sup> Four additional RyR1 backbone chimeras were constructed; they contain either of the two EF-hands (R41 and R51), both (R41'), or neither (R51'), from the RyR2 sequence. The R51' chimera showed essentially the same  $Ca^{2+}$  activation and inactivation profiles as WT RyR1 (Figure 2B). The R41 chimera, which contains only EF2 from the RyR2 sequence, had a slight increase in IC<sub>50</sub> compared with that of WT RyR1, but the difference was not significant in the absence of  $Mg^{2+}$ . In contrast, the R41' chimera, containing both EF1 and EF2 of RyR2, and R51, carrying only EF1 from RyR2, showed significantly increased IC<sub>50</sub> values. These  $Ca^{2+}$ -dependent inactivation curves were similar with that of the R21 chimera (IC<sub>50</sub> values were insignificantly different from that of R21 in the absence of  $Mg^{2+}$ ). An increase in IC<sub>50</sub> for  $Ca^{2+}$  in R41' and R51 chimeras was also observed in the presence of 1 mM  $Mg^{2+}$  (Figure 2A,B). Although the IC<sub>50</sub> of R41 was also significantly increased



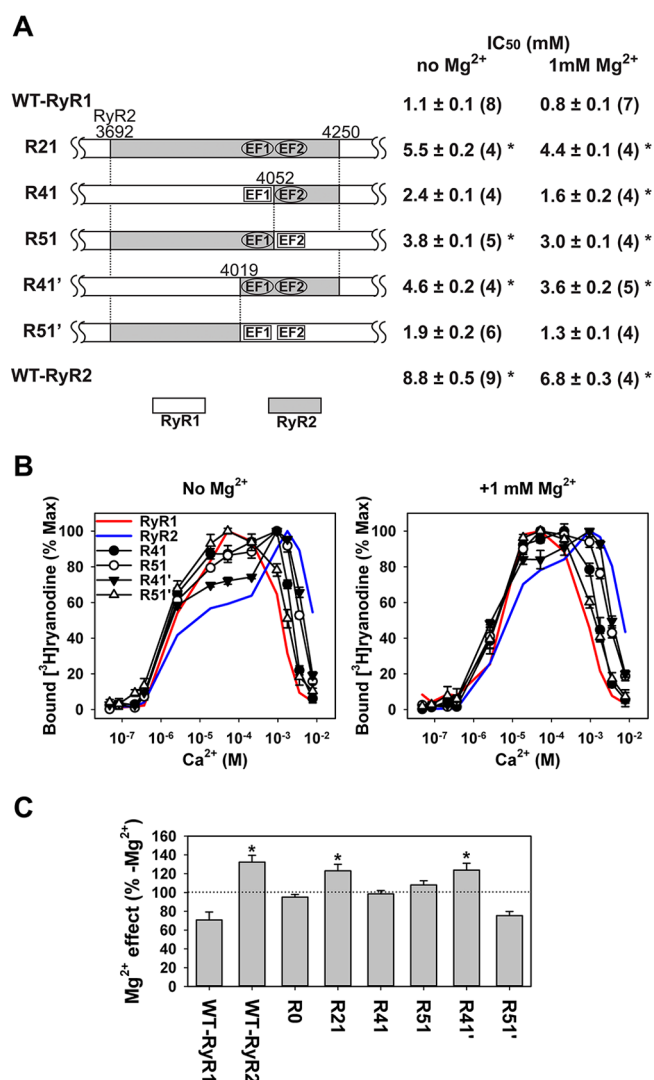


**Figure 2.** EF-hand Ca<sup>2+</sup> binding motifs are critical for Ca<sup>2+</sup>-dependent inactivation and RyR2-specific Mg<sup>2+</sup> activation. (A) Schematic of R41, R51, R41', and R51' chimera channels. IC<sub>50</sub> values are means ± SE of the number of experiments indicated in parentheses. \**p* < 0.05 compared with WT RyR1 (ANOVA followed by Tukey's test among seven groups). (B) Ca<sup>2+</sup>-dependent regulation of R41 (●), R51 (○), R41' (▼), and R51' (△) chimeras in the absence (left) or presence (right) of 1 mM Mg<sup>2+</sup>. Solid red and blue lines represent mean values of WT RyR1 and WT RyR2 from Figure 1A, respectively. Data are means ± SE (*n* = 4–6). (C) Effect of 1 mM Mg<sup>2+</sup> on WT and chimera RyRs. Data are means ± SE (*n* = 4–12). \*Significant activation (*p* < 0.05) compared to no Mg<sup>2+</sup>.

in the presence of 1 mM Mg<sup>2+</sup> compared with that of WT RyR1, the change was only modest as compared with the IC<sub>50</sub> values of R41' and R51 (Figure 2A). The results indicate that the EF-hand Ca<sup>2+</sup> binding domain, especially the N-terminal EF-hand (EF1), is a strong determinant for Ca<sup>2+</sup>-dependent inactivation of RyR. Among these four chimera channels, activities of R41' and possibly R51 chimeras were suppressed with 10–100 μM Ca<sup>2+</sup> (Figure 2B, left panel). The R41' chimera was significantly activated by 1 mM Mg<sup>2+</sup> at 100 μM Ca<sup>2+</sup> (Figure 2C). The R51 chimera was subtly but insignificantly activated, and R41 and R51' chimeras were not activated (Figure 2C). The results suggest that EF-hand Ca<sup>2+</sup> binding sites are critical for the suppression of recombinant RyR2 at 10–100 μM Ca<sup>2+</sup>, which is relieved by 1 mM Mg<sup>2+</sup>.

**Transmembrane and Cytoplasmic Loop Regions Involved in Ca<sup>2+</sup>-Dependent Inactivation.** The last 700 amino acids of RyR2, located in the R0 chimera channel, were further divided into two regions (Figure 3A). According to the

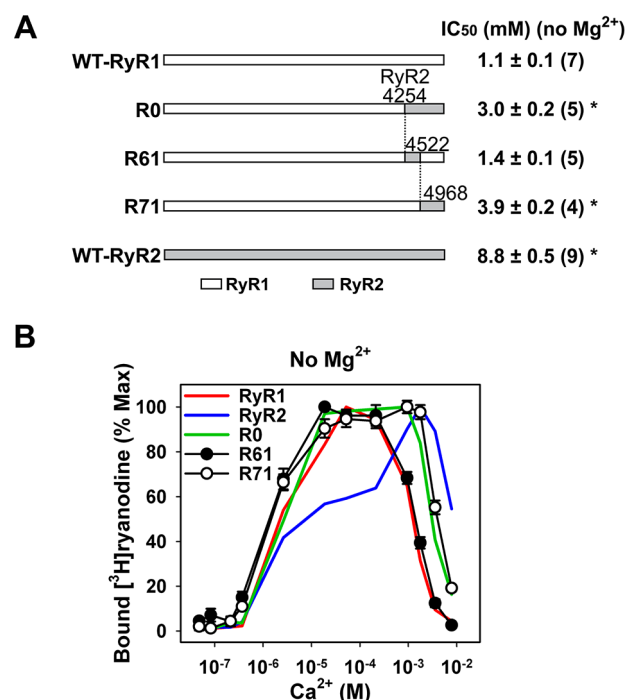


**Figure 3.** C-Terminal end that involves another important region for Ca<sup>2+</sup>-dependent inactivation. (A) Schematic of R61 and R71 chimera channels. IC<sub>50</sub> values are means ± SE of the number of experiments shown in parentheses. \**p* < 0.05 compared with WT RyR1 (ANOVA followed by Tukey's test among five groups). (B) Ca<sup>2+</sup>-dependent regulation of R61 (●) and R71 (○) chimeras in the absence of Mg<sup>2+</sup>. Solid red, blue, and green lines represent mean values of WT RyR1, WT RyR2, and the R0 chimera, respectively (from Figure 1A,C). Data are means ± SE (*n* = 4–5).

bioinformatic sequence analysis and biochemical studies, the region most likely contains six transmembrane domains<sup>26,27</sup> (see also Figure 4A). The R61 chimera (RyR1 amino acids 1–4301 and 4582–5037; RyR2 amino acids 4254–4521) carries a divergent cytoplasmic domain (~25% homologous) and the first transmembrane segment from RyR2, and the R71 chimera (RyR1 amino acids 1–4581; RyR2 amino acids 4522–4968) contains five other RyR2 transmembrane segments together with two cytoplasmic loops (S2–S3 and S4–S5) and the C-terminal tail. Ca<sup>2+</sup>-dependent activation and inactivation curves indicated that R61 was essentially the same as WT RyR1, whereas the IC<sub>50</sub> of R71 significantly increased similar to that of the R0 chimera (Figure 3B). Neither chimera seemed to be suppressed at 10–100 μM Ca<sup>2+</sup>, which is consistent with the R0 chimera (Figures 1C, 2C, and 3B). The results indicate that the last 450 amino acids form another critical region for isoform-specific Ca<sup>2+</sup>-dependent inactivation.

In the R71 chimera region, the N-terminal half (RyR2 amino acids 4522–4780) is more divergent (65% identical) than the C-terminal half (RyR2 amino acids 4781–4968; 93% identical). Therefore, we further constructed eight chimera RyR channels to identify which transmembrane region, cytoplasmic loop, or combination of both in the N-terminal half is important for Ca<sup>2+</sup>-dependent inactivation (Figure 4A,B). As shown in Figure

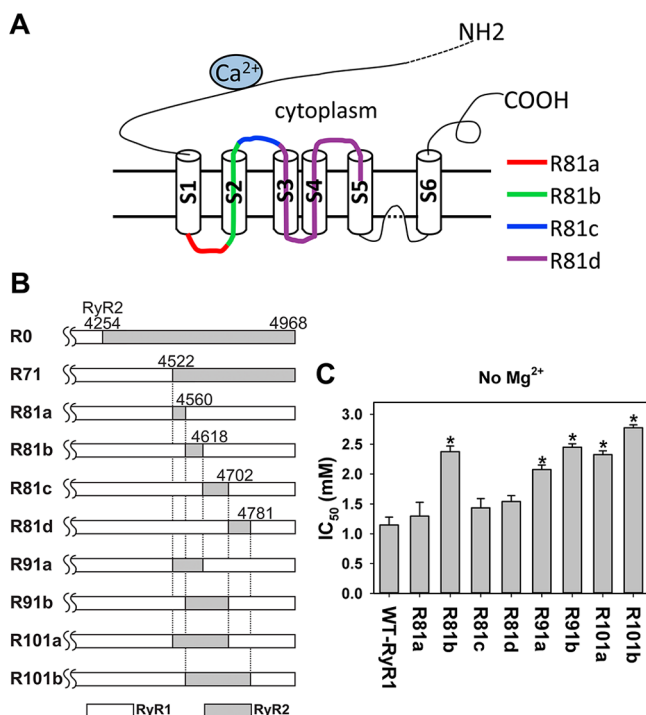


**Figure 4.** Second putative transmembrane region that is a critical determinant for  $\text{Ca}^{2+}$ -dependent inactivation of RyRs. (A) Proposed six-transmembrane model of RyRs. The replaced regions in a series of the R81 chimeras are highlighted with a different color. (B) Schematic of the series of R81, R91, and R101 chimeras. (C)  $\text{IC}_{50}$  values of chimeras are means  $\pm$  SE ( $n = 4-8$ ). \* $p < 0.05$  compared with WT RyR1 (ANOVA followed by Tukey's test among nine groups).

4C, the R81b chimera (RyR1 amino acids 1–4629 and 4688–5037; RyR2 amino acids 4560–4617), carrying the S2 transmembrane of RyR2, showed a higher  $\text{IC}_{50}$  than WT RyR1, and other chimeras containing S2 of RyR2 also had increased  $\text{IC}_{50}$  values.

Two additional chimeras, R121b and R131b, were constructed to assess whether the two regions are sufficient for RyR2-type  $\text{Ca}^{2+}$ -dependent inactivation (Figure 5A). These chimeras carry RyR2 domains of the S2 transmembrane (R81b) or S2 transmembrane with the S2–S3 cytoplasmic loop (R91b) in addition to the RyR2 EF-hand region identified in the R41' chimera.  $\text{Ca}^{2+}$ -dependent inactivation of both chimeras was essentially the same as that of WT RyR2 (Figure 5B), which suggests that two distinct regions of RyR are sufficient for isoform-specific  $\text{Ca}^{2+}$ -dependent inactivation. One region contains two EF-hand  $\text{Ca}^{2+}$  binding motifs, and the other is the second transmembrane segment and possibly its flanking region. Activities of both R121b and R131b chimeras were suppressed at  $10-100 \mu\text{M}$   $\text{Ca}^{2+}$  (Figure 5B), which is consistent with the involvement of RyR2-type EF-hands (R41' region). Consistently, both R121b and R131b were activated by  $1 \text{ mM}$   $\text{Mg}^{2+}$  at  $100 \mu\text{M}$   $\text{Ca}^{2+}$  (Figure 5C).

## DISCUSSION

Previous studies with RyR1–RyR2 chimeras have indicated that the C-terminal quarter of RyRs is crucial for  $\text{Ca}^{2+}$ -dependent inactivation.<sup>15,16</sup> Du et al.<sup>15</sup> showed that the replacement of any one of the three RyR1 domains located in the C-terminal quarter with corresponding RyR2 domains increased the  $\text{IC}_{50}$  for  $\text{Ca}^{2+}$  (Figure 6). Furthermore, the region corresponding to

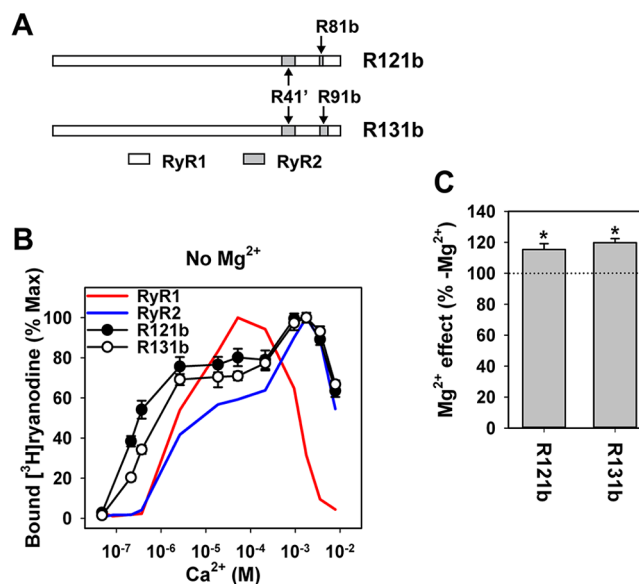


**Figure 5.** Two RyR2 domains are sufficient for RyR2-type  $\text{Ca}^{2+}$ -dependent inactivation. (A) Schematic of R121b and R131b chimeras. (B)  $\text{Ca}^{2+}$ -dependent activity changes of R121b (●) and R131b (○) chimeras in the absence of  $\text{Mg}^{2+}$ . Solid red and blue lines represent mean values of WT RyR1 and WT RyR2, respectively, from Figure 1A.  $\text{IC}_{50}$  values of R121b and R131b are  $11.2 \pm 1.3$  and  $12.3 \pm 0.7 \text{ mM}$ , respectively. Data are means  $\pm$  SE ( $n = 5$ ). (C) Effect of  $1 \text{ mM}$   $\text{Mg}^{2+}$  on R121b and R131b chimeras. Data are means  $\pm$  SE ( $n = 4-5$ ). \*Significant activation ( $p < 0.05$ ) compared with no  $\text{Mg}^{2+}$ .

RyR2 amino acids 4143–4334 represented the middle domain<sup>28</sup> (Figure 6). Our current results with RyR1 backbone chimeras clearly demonstrated that two distinct regions, the EF-hand domain and the second transmembrane segment (S2) in RyR1, are required for high-affinity  $\text{Ca}^{2+}$ -dependent inactivation ( $\sim 1 \text{ mM}$ ). Both regions are involved in the domains that have been described in the previous papers (Figure 6). Although studies with RyR2–backbone chimeras remain to be performed, our current studies succeeded in narrowing the regions responsible for  $\text{Ca}^{2+}$ -dependent inactivation of RyR1.

We also calculated the gain of activity of each chimera by normalizing the peak values of  $\text{Ca}^{2+}$ -dependent activity to  $B_{\text{max}}$  values (Table S1 of the Supporting Information). It was reported that RyR1 activity was suppressed in the native skeletal muscle membrane fraction, whereas RyR2 activity was relatively high.<sup>29,30</sup> In the study presented here, we observed that the average WT RyR2 activity is higher than that of WT RyR1, but with a less pronounced difference. It is possible that a lack of accessory proteins such as FK506-binding proteins,<sup>29</sup> and addition of oxidized glutathione, which specifically regulates RyR1 in the recombinant system,<sup>31</sup> minimized the difference.

The deletion of the negatively charged region (RyR1 amino acids 1872–1923), known as the D3 divergent region, from RyR1 reduced the affinity for  $\text{Ca}^{2+}$ -dependent inactivation by 3-fold.<sup>32</sup> However, a RyR1 backbone chimera carrying the D3 region of RyR2 was inhibited by  $\text{Ca}^{2+}$  with an affinity similar to that of WT RyR1.<sup>15</sup> Therefore, deleting a large S2-amino acid sequence possibly caused a conformational change, allosterically affecting  $\text{Ca}^{2+}$ -dependent inactivation rather than highlighting the difference between  $\text{Ca}^{2+}$ -dependent inactivation of RyR1 and RyR2.

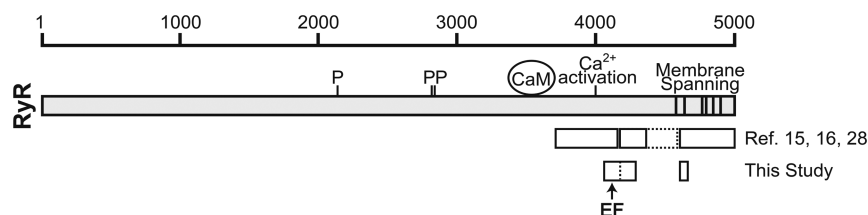


**Figure 6.** Diagram of domains for  $\text{Ca}^{2+}$ -dependent inactivation. Sequence domains suggested by RyR1–RyR2 chimera analyses in previous work<sup>15,16,28</sup> and this study are shown as open boxes together with other identified regulatory domains.<sup>3,4</sup> EF denotes the position of two EF-hand  $\text{Ca}^{2+}$  binding sites. P indicates three potential phosphorylation sites. CaM represents calmodulin.

Our results suggest that the EF-hand domain is most likely a sensor for  $\text{Ca}^{2+}$ -dependent inactivation. The  $\text{Ca}^{2+}$  binding signal could be transmitted to the transmembrane effector site, possibly located in S2. Ikemoto and colleagues proposed that an interdomain interaction between the N-terminal and central domains of RyR1 is crucial for channel regulation.<sup>33</sup> Such a regulatory mechanism may fit with this long-range interaction; that is, the conformation of the interaction between the EF-hand domain and the S2 segment (or possibly their flanking regions) is changed upon binding of  $\text{Ca}^{2+}$  to EF-hands. Studies that include determination of the proximity between domains by FRET measurements<sup>34</sup> and three-dimensional structure analysis<sup>35</sup> and direct monitoring of domain–domain interaction<sup>33</sup> need to be performed to test this hypothesis. Affinities of  $\text{Ca}^{2+}$  for recombinant RyR1 and RyR2 EF-hand domains were similar in the equilibrium binding experiments,<sup>8</sup> which does not explain the difference in  $\text{Ca}^{2+}$ -dependent inactivation of RyR1 and RyR2 channel activities. A possible explanation is that the affinities of domain interactions are different, which affects isoform-specific  $\text{Ca}^{2+}$ -dependent inactivation.

Fessenden et al.<sup>10</sup> scrambled amino acid sequences of EF1 and EF2 in full-length RyR1 and expressed the mutant RyR1s in 1B5 RyR-deficient myotubes for functional characterization. They found that the EF1-scrambled mutant showed an ~2-fold increase in its  $\text{IC}_{50}$  for  $\text{Ca}^{2+}$ . These results are in good agreement with the study presented here that EF1 is important for  $\text{Ca}^{2+}$ -dependent inactivation (Figure 2A).

It should be noted that the  $\text{EC}_{50}$  values for  $\text{Ca}^{2+}$  of R41' and R81b chimeras were not essentially different from that of WT RyR1 (Table 1 and Figure 3B, R81b,  $\text{Ca}^{2+}$ -dependent activity change not shown). However, the chimera carrying both RyR2 regions, the R121b chimera, was substantially activated by a lower concentration of  $\text{Ca}^{2+}$  compared to WT RyR1 (Figure 4C). A similar effect was observed in the R131b chimera, which carries the R41' and R91b chimeric region of RyR2. The same effects were observed in earlier studies with RyR1–RyR2 chimera channels.<sup>15</sup> As discussed, a conformational change in chimera channels may affect channel activation. Nevertheless, we found that  $\text{Ca}^{2+}$ -dependent inactivation of R121b and R131b were additives of R41' and R81b or R91b, which most likely indicates the importance of two domains in  $\text{Ca}^{2+}$ -dependent inactivation.

It was reported that the activities of RyR2 in rat ventricular muscle, as well as in recombinant rabbit RyR2, were suppressed at 10–100  $\mu\text{M}$   $\text{Ca}^{2+}$ , and the suppression was relieved by 1 mM  $\text{Mg}^{2+}$ . It is perhaps due to the conformational change during sample preparation or the lack of accessory proteins; a different preparation with RyR2 from rabbit ventricular muscle was not activated by  $\text{Mg}^{2+}$ .<sup>19</sup> In this study, we confirmed this effect on recombinant RyR2 and found that the recombinant rabbit RyR1 was not activated by  $\text{Mg}^{2+}$ . Although the physiological

significance of the effect remains unknown, we found that the EF-hand region of RyR2 is responsible for this effect. It is conceivable that binding of  $\text{Mg}^{2+}$  to the EF-hand  $\text{Ca}^{2+}$  binding sites at physiological concentrations (0.5–1 mM) stabilizes the channel conformation and renders them more sensitive to  $\text{Ca}^{2+}$  activation and other modulators.

In summary, we advanced our understanding of the structure–function aspect of  $\text{Ca}^{2+}$ -dependent inactivation of RyRs. Our results suggest that calcium ions bind to EF-hand regions and the functional signal is transmitted to the effector site (possible inactivation gate) in the second transmembrane segment. Thus, further studies for narrowing the region, ideally at the single-amino acid level, will lead us to define the molecular structure of the inactivation gate of RyRs.

## ■ ASSOCIATED CONTENT

### § Supporting Information

Figure S1 and Table S1. This material is available free of charge via the Internet at <http://pubs.acs.org>.

## ■ AUTHOR INFORMATION

### Corresponding Author

\*Department of Regenerative Medicine and Cell Biology, Medical University of South Carolina, 173 Ashley Ave., Basic Science Building 601, MSC 508, Charleston, SC 29425. E-mail: [yamaguch@musc.edu](mailto:yamaguch@musc.edu). Phone: (843) 876-2487. Fax: (843) 792-0664.

### Funding

The studies were supported by National Institutes of Health Grant R03AR061030, American Heart Association Grant 10SDG3500001, and National Science Foundation Grant EPS0903795 to N.Y.

### Notes

The authors declare no competing financial interest.

## ■ ACKNOWLEDGMENTS

We thank Gerhard Meissner for his advice on chimera constructs and Timothy Holford for technical assistance and suggestions.

## ■ ABBREVIATIONS

$\text{EC}_{50}$ , half-maximal effective concentration; HEK, human embryonic kidney;  $\text{IC}_{50}$ , half-maximal inhibitory concentration; RyR, ryanodine receptor; RyR1, skeletal muscle RyR; RyR2, cardiac muscle RyR; SR, sarcoplasmic reticulum; WT, wild type.

## ■ REFERENCES

- (1) Franzini-Armstrong, C., and Protasi, F. (1997) Ryanodine receptors of striated muscles: A complex channel capable of multiple interactions. *Physiol. Rev.* 77, 699–729.



- (2) Meissner, G. (2002) Regulation of mammalian ryanodine receptors. *Front. Biosci.* 7, d2072–d2080.
- (3) Hamilton, S. L., and Serysheva, I. I. (2009) Ryanodine receptor structure: Progress and challenges. *J. Biol. Chem.* 284, 4047–4051.
- (4) Capes, E. M., Loaiza, R., and Valdivia, H. H. (2011) Ryanodine receptors. *Skeletal Muscle* 1, 18.
- (5) Chen, S. R. W., and MacLennan, D. H. (1994) Identification of calmodulin-,  $\text{Ca}^{2+}$ -, and ruthenium red-binding domains in the  $\text{Ca}^{2+}$  release channel (ryanodine receptor) of rabbit skeletal muscle sarcoplasmic reticulum. *J. Biol. Chem.* 269, 22698–22704.
- (6) Chen, S. R. W., Ebisawa, K., Li, X., and Zhang, L. (1998) Molecular identification of the ryanodine receptor  $\text{Ca}^{2+}$  sensor. *J. Biol. Chem.* 273, 14675–14678.
- (7) Li, P., and Chen, S. R. W. (2001) Molecular basis of  $\text{Ca}^{2+}$  activation of the mouse cardiac  $\text{Ca}^{2+}$  release channel (ryanodine receptor). *J. Gen. Physiol.* 118, 33–44.
- (8) Xiong, H., Feng, X., Gao, L., Xu, L., Pasek, D. A., Seok, J. H., and Meissner, G. (1998) Identification of a two EF-hand  $\text{Ca}^{2+}$  binding domain in lobster skeletal muscle ryanodine receptor/ $\text{Ca}^{2+}$  release channel. *Biochemistry* 37, 4804–4814.
- (9) Xiong, L., Zhang, J. Z., He, R., and Hamilton, S. L. (2006) A  $\text{Ca}^{2+}$ -binding domain in RyR1 that interacts with the calmodulin binding site and modulates channel activity. *Biophys. J.* 90, 173–182.
- (10) Fessenden, J. D., Feng, W., Pessah, I. N., and Allen, P. D. (2004) Mutational analysis of putative calcium binding motifs within the skeletal ryanodine receptor isoform, RyR1. *J. Biol. Chem.* 279, 53028–53035.
- (11) Tripathy, A., and Meissner, G. (1996) Sarcoplasmic reticulum lumenal  $\text{Ca}^{2+}$  has access to cytosolic activation and inactivation sites of skeletal muscle  $\text{Ca}^{2+}$  release channel. *Biophys. J.* 70, 2600–2615.
- (12) Xu, L., and Meissner, G. (1998) Regulation of cardiac muscle  $\text{Ca}^{2+}$  release channel by sarcoplasmic reticulum lumenal  $\text{Ca}^{2+}$ . *Biophys. J.* 75, 2302–2312.
- (13) Liu, W., Pasek, D. A., and Meissner, G. (1998) Modulation of  $\text{Ca}^{2+}$ -gated cardiac muscle  $\text{Ca}^{2+}$ -release channel (ryanodine receptor) by mono- and divalent ions. *Am. J. Physiol.* 274, C120–C128.
- (14) Meissner, G., Rios, E., Tripathy, A., and Pasek, D. A. (1997) Regulation of skeletal muscle  $\text{Ca}^{2+}$  release channel (ryanodine receptor) by  $\text{Ca}^{2+}$  and monovalent cations and anions. *J. Biol. Chem.* 272, 1628–1638.
- (15) Du, G. G., and MacLennan, D. H. (1999)  $\text{Ca}^{2+}$  inactivation sites are located in the COOH-terminal quarter of recombinant rabbit skeletal muscle  $\text{Ca}^{2+}$  release channels (ryanodine receptors). *J. Biol. Chem.* 274, 26120–26126.
- (16) Nakai, J., Gao, L., Xu, L., Xin, C., Pasek, D. A., and Meissner, G. (1999) Evidence for a role of C-terminus in  $\text{Ca}^{2+}$  inactivation of skeletal muscle  $\text{Ca}^{2+}$  release channel (ryanodine receptor). *FEBS Lett.* 459, 154–158.
- (17) Laver, D. R., Baynes, T. M., and Dulhunty, A. F. (1997) Magnesium inhibition of ryanodine-receptor calcium channels: Evidence for two independent mechanisms. *J. Membr. Biol.* 156, 213–229.
- (18) Murayama, T., Kurebayashi, N., and Ogawa, Y. (2000) Role of  $\text{Mg}^{2+}$  in  $\text{Ca}^{2+}$ -induced  $\text{Ca}^{2+}$  release through ryanodine receptors of frog skeletal muscle: Modulations by adenine nucleotides and caffeine. *Biophys. J.* 78, 1810–1824.
- (19) Chugun, A., Sato, O., Takeshima, H., and Ogawa, Y. (2007)  $\text{Mg}^{2+}$  activates the ryanodine receptor type 2 (RyR2) at intermediate  $\text{Ca}^{2+}$  concentrations. *Am. J. Physiol.* 292, C535–C544.
- (20) Takashima, H., Nishimura, S., Matsumoto, T., Ishida, H., Kangawa, K., Minamino, N., Matsuo, H., Ueda, M., Hanaoka, M., Hirose, T., and Numa, S. (1989) Primary structure and expression from complementary DNA of skeletal muscle ryanodine receptor. *Nature* 339, 439–445.
- (21) Nakai, J., Imagawa, T., Hakamata, Y., Shigekawa, M., Takeshima, H., and Numa, S. (1990) Primary structure and functional expression from cDNA of the cardiac ryanodine receptor/calcium release channel. *FEBS Lett.* 271, 169–177.
- (22) Yamaguchi, N., Xu, L., Pasek, D. A., Evans, K. E., Chen, S. R. W., and Meissner, G. (2005) Calmodulin regulation and identification of calmodulin binding region of type-3 ryanodine receptor calcium release channel. *Biochemistry* 44, 15074–15081.
- (23) Yamaguchi, N., Xu, L., Pasek, D. A., Evans, K. E., and Meissner, G. (2003) Molecular basis of calmodulin binding to cardiac muscle  $\text{Ca}^{2+}$  release channel (ryanodine receptor). *J. Biol. Chem.* 278, 23480–23486.
- (24) Schoenmakers, T. J., Visser, G. J., Flik, G., and Theuvsen, A. P. (1992) CHELATOR: An improved method for computing metal ion concentrations in physiological solutions. *BioTechniques* 12, 870–879.
- (25) Sutko, J. L., Airey, J. A., Welch, W., and Ruest, L. (1997) The pharmacology of ryanodine and related compounds. *Pharmacol. Rev.* 49, 53–98.
- (26) Du, G. G., Sandhu, B., Khanna, V. K., Guo, X. H., and MacLennan, D. H. (2002) Topology of the  $\text{Ca}^{2+}$  release channel of skeletal muscle sarcoplasmic reticulum (RyR1). *Proc. Natl. Acad. Sci. U.S.A.* 99, 16725–16730.
- (27) Ramachandran, S., Chakraborty, A., Xu, L., Mei, Y., Samsó, M., Dokholyan, N. V., and Meissner, G. (2013) Structural determinants of skeletal muscle ryanodine receptor gating. *J. Biol. Chem.* 288, 6154–6165.
- (28) Du, G. G., Khanna, V. K., and MacLennan, D. H. (2000) Mutation of divergent region 1 alters caffeine and  $\text{Ca}^{2+}$  sensitivity of the skeletal muscle  $\text{Ca}^{2+}$  release channel (ryanodine receptor). *J. Biol. Chem.* 275, 11778–11783.
- (29) Murayama, T., and Ogawa, Y. (2004) RyR1 exhibits lower gain of CICR activity than RyR3 in the SR: Evidence for selective stabilization of RyR1 channel. *Am. J. Physiol.* 287, C36–C45.
- (30) Murayama, T., and Kurebayashi, N. (2011) Two ryanodine receptor isoforms in nonmammalian vertebrate skeletal muscle: Possible roles in excitation-contraction coupling and other processes. *Prog. Biophys. Mol. Biol.* 105, 134–144.
- (31) Petrochenko, E. V., Yamaguchi, N., Pasek, D. A., Borchers, C. H., and Meissner, G. (2011) Mass spectrometric analysis and mutagenesis predict involvement of multiple cysteines in redox regulation of the skeletal muscle ryanodine receptor ion channel complex. *Res. Rep. Biol.* 2011, 13–21.
- (32) Hayek, S. M., Zhu, X., Bhat, M. B., Zhao, J., Takeshima, H., Valdivia, H. H., and Ma, J. (2000) Characterization of a calcium-regulation domain of the skeletal-muscle ryanodine receptor. *Biochem. J.* 351, 57–65.
- (33) Ikemoto, N., and Yamamoto, T. (2002) Regulation of calcium release by interdomain interaction within ryanodine receptors. *Front. Biosci.* 7, d671–d683.
- (34) Raina, S. A., Tsai, J., Samsó, M., and Fessenden, J. D. (2012) FRET-based localization of fluorescent protein insertions within the ryanodine receptor type 1. *PLoS One* 7, e38594.
- (35) Wang, R., Zhong, X., Meng, X., Koop, A., Tian, X., Jones, P. P., Fruen, B. R., Wagenknecht, T., Liu, Z., and Chen, S. R. W. (2011) Localization of the dantrolene-binding sequence near the FK506-binding protein-binding site in the three-dimensional structure of the ryanodine receptor. *J. Biol. Chem.* 286, 12202–12212.